Proceedings of the 1996 IEEE
International Conference on Robotics and Automation
Minneapolis, Minnesota - April 1996

Vibration Control of Deployment Structures' Long-Reach Space Manipulators: The P-PED Method

Miguel A. Torres*, Steven Dubowsky† and Attilio C. Pisoni‡

Abstract

This paper presents a control method called Pseudo-Passive Energy Dissipation (P-PED) method. The P-PED method is a closed-loop control scheme for increasing the overall damping characteristics of an elastically-mounted space manipulator system. It reduces degrading base vibrations resulting from external disturbances or motion of the manipulator, thereby decreasing the time necessary to perform maneuvers. A methodology for computing the optimal P-PED gains is presented. Experimental results are presented which show that the P-PED method is viable for practical implementation.

1 Introduction

Telerobotic manipulator systems have been proposed as an alternative to costly and hazardous Extra Vehicular Activities [23,15]. These proposed systems are expected to perform a variety of tasks, such as satellite servicing and space structure assembly . An example of a proposed space manipulator system is the Special Purpose Dextrous Manipulator (SPDM used with the proposed Space Station Remote Manipulator System SSRMS) [13,11]. This system is designed so that the very large, low-bandwidth and less accurate SSRMS will provide a large working envelope while the smaller, higher-bandwidth and more accurate SPDM will provide fast, precise motions and forces.

Based on current design specifications, vibration problems are expected with the SSRMS, particularly when it is excited by the two-arm 19 degree-of-freedom (DOF) SPDM. Operating the SPDM slowly does reduce the amount of vibration produced by the maneuver, but at the cost of reducing the overall system effectiveness by greatly increasing the time required to perform tasks. Consequently, before space manipulator systems such as the SSRMS and the SPDM are deployed, reliable and effective methods for modelling, controlling and planning the motion of these systems must be developed.

In many tasks the large SSRMS will be stationary, its joints locked, while the small SPDM performs its functions. This mode of operation will allow the system to be modelled as a rigid redundant manipulator mounted on a highly flexible supporting structure. Research on the dynamics and control of space robotic systems has largely focuses on free-floating or free-flying space manipulators [8,10]. Extensive research have been conducted on the dynamics and control of flexible-link manipulators in terrestrial or industrial settings [2]. Prefiltering techniques and end-point control have been proposed for this problem. [14, 4]. The problem of manipulators mounted on highly flexible bases has received less attention. End-point motion control using base motion measurements has been proposed [12]. An optimum path planning algorithm to reduce the vibrations in elastically constrained space manipulator systems has also been proposed [19, 20, 22].

This paper presents a method for tuning the manipulator's closed loop gains so as to maximize the transfer of energy from the manipulator's flexible supporting structure to its actuators. This energy is then dissipated by the actuators since they are commanded to behave as passive linear springs and dampers. The algorithm is given the name Pseudo-Passive Energy Dissipation (P-PED) method, indicating that passive elements such as springs and dampers are used to damp out the structure vibration, but they are implemented using active elements, namely the joint control system and the actuators. A method for choosing configurations of the manipulators so that the P-PED method can be used more effectively has also been developed; but a discussion of this is beyond the scope of this paper, but can be found in [19,21].

This paper presents numerical as well as experimental evaluation of the P-PED method. The experiments were conducted on two planar microgravity laboratory systems: the MIT Elastic Base Manipulator Testbed and the Martin Marietta Harmonic Drive Planar Arm System. The results of this evaluation demonstrate the effectiveness of the P-PED method in reducing the vibrations of the supporting structure due to motion of the supported manipulator.

2 Analytical Development

2.1 System Dynamic Model

Figure 2 shows a model of an n degree-of-freedom (DOF) rigid body manipulator mounted on a flexible base in a zero gravity environment. The flexible base is modelled by a six DOF linear structure. The distributed mass of the supporting structure is assumed

*Assistant professor, Dept. of Mechanical Engineering, University of Puerto Rico - RUM, Mayagüez, PR, formally graduate research assistant, MIT

†Professor, Dept. of Mechanical Engineering, Massachusetts Institute of Technology, Cambridge MA

‡Department of Mechanical Engineering, University of Ancona, Italy, formally research assistant, Dept. of Mechanical Engineering, MIT

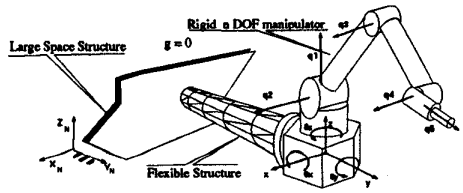

Figure 1: Elastically Constrained Space Manipulator Dynamic Model

to be small compared to the mass of the manipulator and its base. A set of generalized coordinates is defined as $\xi = [\phi, q]^T$. $\phi = (x, y, z, \theta_x, \theta_y, \theta_z)$ represents the 6 generalized coordinates describing the position and orientation of the manipulator's base frame with respect to a Newtonian reference frame. The n-element vector $q = (q_1, q_2, \ldots, q_n)$ represents the n manipulator joint displacements. A corresponding generalized force vector is defined as $\Xi = [\tau_\phi, \tau_q]^T$, and the system equations of motion are written as:

$$H(\xi)\ddot{\xi} + C(\xi, \dot{\xi})\dot{\xi} + K\xi = \Xi \qquad (1)$$

where $H(\xi) \in \Re^{n+6 \times n+6}$ is a symmetric, positive-definite inertia matrix, $C(\xi, \dot{\xi})\dot{\xi} \in \Re^{n+6}$ is a force/torque vector accounting for centrifugal and Coriolis effects, and

$$K = \begin{Bmatrix} K_b & 0 \\ 0 & 0 \end{Bmatrix} \in \Re^{n+6 \times n+6} \qquad (2)$$

is a symmetric matrix representing the stiffness of the system. The 6 by 6 K_b submatrix is the stiffness matrix of the supporting structure.

2.2 The Pseudo-Passive Energy Dissipation Method

The Pseudo-Passive Energy Dissipation method is a closed loop control scheme designed to use the manipulator actuators to damp the vibrations of the supporting structure. In addition to the losses due to friction at the joints, energy is dissipated through the actuators when they are made to behave as linear dampers through what is known as derivative control, similar to a common technique used to increase the stability margins of a dynamic system [7]. However, in order for the energy contained in the vibratory modes of the base to be most effectively transferred to the manipulators actuators, the closed loop gains of the manipulator joints must be carefully selected.

If the joints are controlled with a proportional-derivative (PD) controller whose gains are selected to satisfy a high-bandwidth performance specification, then the manipulator will not effectively damp out base vibrations. In fact, with such a high-bandwidth controller, motion of the manipulator will excite vibrations in its supporting structure. This is because, once the maneuver is completed, the high bandwidth characteristics of the manipulator make it behaves as a rigid body relative to the slowly vibrating supporting structure.

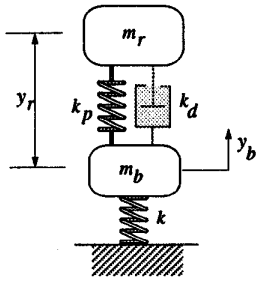

Figure 2: A Two-DOF Mass-Spring-Damper System

Therefore it is proposed that when the manipulator is required to damp supporting structure vibrations, such as after the manipulator has moved to a specific configuration, its gains are tuned to match the impedance of the manipulator system with the impedance of the base, thus maximizing the transfer of energy from the manipulator's supporting structure to the manipulator itself where it is dissipated. This control is called P-PED control.

One way of computing the P-PED gains for a given manipulator/base system is to linearize the full dynamics of the given manipulator/base system and to use an iterative searching algorithm to search for joint gains that maximize the damping characteristics of the system [5]. Unfortunately, this method becomes computationally intensive for real systems, i.e., many DOF. A more efficient method for computing the P-PED gains for a given manipulator is proposed in this paper. The proposed method also lend itself to real-time computation of the P-PED gains and provides an insight into the dynamic behavior of the system.

2.3 Computing the P-PED Gains

A simple two-mass system, see Figure 3, is used in the following development to illustrate the technique for computing the P-PED gains and to give insight into the dynamic behavior of the system under P-PED control. This method is then generalized to an arbitrary n-DOF system mounted on a linear compliant structure such as shown in Figure 2.

2.3.1 Root Locus Analysis

Consider the simple two-DOF mass-spring-damper system shown in Figure 3. This system can be thought of as representing a very simple flexibly supporting manipulator. The mass m_r represents the total mass of the robot and m_b the mass of the system's base. In a similar fashion, k_p and k_d can be seen as the stiffness and damping effect caused by the the proportional and derivative P-PED gains of the manipulator joints on the system, respectively. The unforced dynamic of this system can be represented by the homogeneous differential equation

$$\dot{x} = Ax \qquad (3)$$

where $x = [y_b, y_r, \dot{y}_b, \dot{y}_r]^T$ and A is the system matrix given by

$$A = \begin{Bmatrix} 0 & 0 & 1 & 0 \\ 0 & 0 & 0 & 1 \\ -\frac{k}{m_b} & \frac{k_p}{m_b} & -\frac{b}{m_b} & \frac{k_d}{m_b} \\ \frac{k}{m_b} & -(\frac{k_p}{m_r}+\frac{k_P}{m_b}) & \frac{b}{m_b} & -(\frac{k_d}{m_r}+\frac{k_d}{m_b}) \end{Bmatrix} \quad (4)$$

For the system shown in Figure 3, there is a unique set of values for k_p and k_d that maximizes the damping of the system dominant poles. See reference [19,21]. The following is an iterative procedure to find these values that have been found in practice to converge very rapidly.

First, set k_P equals zero in Equation (4) and use the root locus methodology to determine a best value for k_d. This value corresponds to the highest value of k_d that gives the highest damping to the system. Second, fix k_d at this value and use a root locus plot again, this time varying k_p until a value for k_p is obtained. This process is repeated always increasing the values of k_d and k_p in each step until they can no longer be increased and improve system stability.

2.3.2 Kinematic Analysis

As mentioned, the system depicted in Figure 3 represents a simplified dynamic model of a flexible base manipulator system, where m_r represents the total mass of the manipulator and its payload, and m_b represents the mass of the system's base. The motion of m_r with respect to m_b in Figure 3 can be seen to represent the motion of the manipulator's center of mass with respect to its base. The spring and damper between the two masses in the system in Figure 3 represent the effective spring-damping characteristics present when the joint PD gains are active. In order to compute the manipulator joint P-PED gains that result in the effective dynamic behavior exhibited by k_p and k_d in the model in Figure 3, the values of k_p and k_d need to be translated into the manipulator joints. This can be done effectively by using the Virtual Manipulator [22].

The Virtual Manipulator concept was originally conceived for free-floating space manipulator system and therefore it assumes no external forces acting on the system. The system we are analysing is attached to a compliant structure and therefore there will be external forces acting of on the system. For the Virtual manipulator analysis to be valid in this type of system forces acting of the system's base must be small, the total mass of the manipulator, not counting its base is large and the stiffness of the compliant structure must be low. Given there three conditions the Virtual Manipulator can be used for computing P-PED gains.

First, a virtual manipulator is constructed for the system as shown in Figure 4. For this virtual manipulator the kinematic chain starts at the manipulator's center of mass (Virtual Ground, [22]) and its end-effector is chosen to be at the manipulator's base where it attaches to the compliant structure. The virtual manipulator is a massless kinematic chain whose joint axes are always parallel to the real system's joint

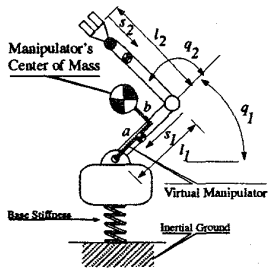

Figure 3: Two-Link Elastically Constrained System

axes and whose base, it virtual ground, coincides with the manipulator's center of mass. This virtual manipulator simplifies the analysis considerably, since now we can view at the virtual system as a massless kinematic chain holding a payload of a mass equal to the total mass of the real manipulator. This model has the same structure as the one depicted in Figure 3.

For the system shown in Figure 4, the dimensions of the links of the virtual manipulator are obtained by using the Virtual Manipulator technique and are [22]:

$$\begin{aligned} a &= \frac{m_1(l_1-s_1)+m_2 l_1}{m_1+m_2} \\ b &= \frac{m_2(l_2-s_2)}{m_1+m_2} \end{aligned} \quad (5)$$

It can be shown that the joints of the virtual manipulator are always parallel to the real system's joint axes and the expression for the virtual manipulator Jacobian, or J_{cm}, is similar to the real system Jacobian, J. The only difference is the length of the links. In this case, the Jacobian for the virtual manipulator is given by

$$J_{cm} = \begin{Bmatrix} -a\sin(q_1) - b\sin(q_1+q_2) & -b\sin(q_1+q_2) \\ a\cos(q_1) + b\cos(q_1+q_2) & b\cos(q_1+q_2) \end{Bmatrix} \quad (6)$$

The subscript in J_{cm} indicates that this expression relates motion of the manipulator joints to motion of the manipulator's center of mass.

$$\dot{X}_{cm} = J_{cm}\dot{q} \quad (7)$$

In general, the manipulator Jacobian also relates force and torque acting on the manipulator's end-effector to actuator torques [1]. This is also true for the J_{cm}; however, in this case it relates forces and torques acting on the base and structure, F_{cm}, to the manipulator actuator torques, τ. This relation is given by

$$\tau = J_{cm}^T F_{cm} \quad (8)$$

The forces/torques, F_{cm}, must be small for the Virtual Manipulator concept to apply in this analysis. Now, if the concept of k_p and k_d, as discussed earlier, is generalized to a 3 DOF motion, an expression for F_{cm} can be written as

$$F_{cm} = K_p X_{cm} - K_d \dot{X}_{cm} \quad (9)$$

where $K_p \in \Re^{3\times3}$ and $K_d \in \Re^{3\times3}$ are diagonal positive-definite matrices describing the desired stiffness and damping characteristics, respectively, between the manipulator center of mass and its base. The diagonal elements of the matrices K_p and K_d are computed using the root locus iterative procedure discussed in the previous section.

Combining Equation (8) and Equation (9) yields

$$\tau = J_{cm}^T (K_p X_{cm} - K_d \dot{X}_{cm}) \quad (10)$$

which, combined with Equation (7) and considering only motions of the manipulator around a nominal configuration, yields

$$\tau = J_{cm}^T K_p J_{cm} q_{err} - J_{cm}^T K_d J_{cm} \dot{q} \quad (11)$$

where q_{err} is the joint error vector, or deviation from a stationary nominal configuration.

Equation (11) leads to the expressions for the manipulator's proportional and derivative joint gains as a function of the previously computed K_p and K_d matrices. These expressions are

$$K_{P-PED} = J_{cm}^T K_p J_{cm} \quad (12)$$

and

$$D_{P-PED} = J_{cm}^T K_d J_{cm} \quad (13)$$

where K_{P-PED} and D_{P-PED} are the manipulator P-PED control gain matrices. Notice Equations (12) and (13) provide the expressions for computing K_{P-PED} and D_{P-PED}, respectively, for a general n-DOF manipulator. For the two-DOF example the matrix J_{cm} is $\in \Re^{2\times2}$. For a general spatial n-DOF manipulator the matrix J_{cm} is $\in \Re^{3\times n}$.

Also note that K_{P-PED} and D_{P-PED} are, in general, full matrices. In order to obtain the system dynamic response, as predicted by the root locus analysis, the full K_{P-PED} and D_{P-PED} matrices must be used in the implementation of the control algorithm. Given this condition, this control scheme cannot be fully implemented using simple decoupled PD control. A more comprehensive control architecture is required, in which the position and velocity of the manipulator joints are globally available. For a manipulator with decoupled PD control, using the diagonal values of the matrices K_{P-PED} and D_{P-PED} will give an approximation of the full P-PED implementation.

K_{P-PED} and D_{P-PED} depend on J_{cm}, which, in turn, is a function of the system configuration. For those configurations in which the matrix J_{cm} becomes singular, values for K_{P-PED} and D_{P-PED} that satisfy the required dynamic behavior will not be found. For cases in which the configuration of the manipulator can be arbitrarily selected, the Coupling Map can be used in selecting such configurations [19,21]. The Coupling Map, shown in Figure 5, is an analytical tool to graphically describe the nonlinear dynamic interaction between a space manipulator and its moving base. The lines depicted in Figure 5 are called the /em Minimum Coupling Lines. Their slopes represent

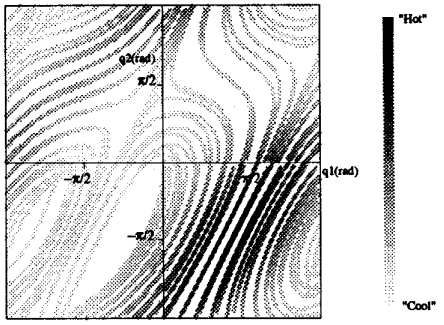

Figure 4: Example of a Coupling Map for a Two DOF Manipulator

local directions in joint space for which motion of the manipulator tangent to these directions will results in relatively low energy transfer to the system's compliant structure. Moving perpendicular to the minimum coupling lines results is relatively high energy transferred between the manipulator and its compliant structure. The relative strength of the coupling for motions perpendicular the the minimum coupling lines depends on the configuration of the manipulator, or its location in joint space. This information is represented in the form of shaded regions. If the configuration of the manipulator can be arbitrarily chosen when damping vibrations while under P-PED control, these configuration must be chosen to lie within one of the dark regions, i.e.,*Hot Spots* in the Coupling Map. See references [21].

3 Experimental Evaluation

3.1 P-PED control for Disturbance Rejection

The first set of experimental results presented here the Martin Marietta Harmonic Drive Manipulator (HDM), see Figure 6,was used to examine the P-PED's ability to damp out vibrations caused be external disturbances. The HDM [16] was designed as a research testbed to study fundamental problems related to the control of space manipulator systems. The HDM is a three-link planar manipulator supported by air bearings on a glass table top for frictionless motion. The actuators are brush DC motors driving an 80:1 harmonic drive transmission. Local joint torque feedback loops allow the arm to behave as a frictionless direct-drive system. Each joint has a motor-side tachometer, an output torque transducer, and a resolver to measure joint angle.

For this experiment the HDM was mounted to a 0.886m aluminum beam which acted as a flexible structure and an accelerometer was mounted at the outer casing of the shoulder joint to monitor base vibrations. Figure 6 shows the overall dimensions of the system including the dimensions of the glass table top and location of the base accelerometer. A 20 lb (9.1 kg) payload was attached to the manipulator wrist joint. For this experiment, only the shoulder and the elbow joints were used in motion planning. The wrist

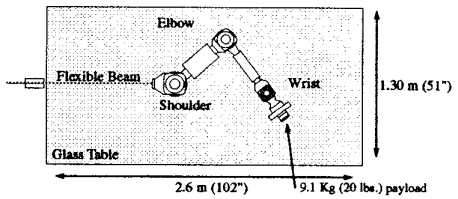

Figure 5: The Martin Marietta Harmonic Drive Planar Arm Testbed

	PD Gains		P-PED Gains	
	Kp	Kd	K_{P-PED}	D_{P-PED}
Joint 1	200.00	7.0	47.27	2.0
Joint 2	200.00	7.0	47.27	0.3

Table 1: Manipulator Gains for PD and P-PED Control

joint was keep locked at the configuration shown in Figure 6. For this configuration, the HDM base vibration was between 0.45 to 0.50 Hz depending on the manipulator configuration. See Reference [19] for a complete description of the HDM system.

Based on the geometric and materials properties of the aluminum beam, the stiffness and damping matrix for the HDM supporting structure were calculated at the end of the beam or base of the manipulator. These are

$$K_b = \begin{Bmatrix} 10,000 & -4,400 \\ -4,400 & 2,600 \end{Bmatrix} \quad (14)$$

and

$$D_b = \begin{Bmatrix} 15.3 & -1.2 \\ -1.2 & 5.3 \end{Bmatrix} \quad (15)$$

For this experiment, the manipulator will be kept at the configuration shown in Figure 6 while a disturbance is applied to its base.

First, the manipulator PD gains were tuned to its nominal high bandwidth values, see Table 1. The system was commanded to maintain its configuration while a disturbance was applied to the base. The acceleration of the base was recorded and is shown in Figure 7. As can be seen the system took more than 20 second to dissipate all the vibrational energy introduced by the disturbance.

Second, the manipulator P-PED gains were computed for this configuration based on the approach described above, the values of the gains shown in Table 1. With the manipulator still commanded to keep its configuration under P-PED control a similar disturbance was applied to the base and the base acceleration was recorded. The results are shown in Figure 8.

Notice that under P-PED control the system was able dissipate the disturbance produced base vibration in only 3 seconds, which was significantly faster than when the system was commanded to keep its position using conventionally tuned PD control, which required more than 20 seconds. See Figure 7

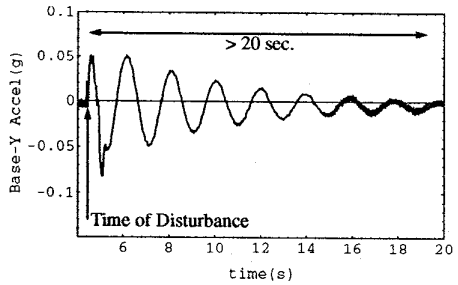

Figure 6: Base Response to an External Disturbance: Conventional PD Control

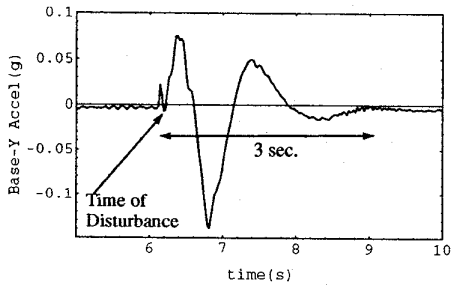

Figure 7: Base Response to an External Disturbance: Under P-PED Control

3.2 P-PED in Fast Maneuvers

For this experiment the MIT Elastic Base Manipulator Testbed (MIT-EBM) was used. The MIT-EBM consist of a two-DOF rigid manipulator mounted on a specially designed flexible base. See Figure 9. The particular design of the MIT-EBM's flexible beam results in a structure with very low stiffness characteristics in bending in the horizontal plane and very high stiffness characteristics in vertical bending and in torsion. This based design results in a 1-DOF flexible base with a natural frequency of about one Hz. The manipulator is 0.5 m long with each of the joints powered by brush DC motors each with a 33.1:1 reduction drive and equipped with an optical encoder at the motor side to measure absolute joint position. A 0.25 Kg payload is attached to the end of the second link. Vibrations induced in the beam are measured with an accelerometer mounted at the base of the manipulator.

The experiment is designed to determine the effectiveness of the P-PED method in damping residual structural vibrations resulting from motion of the manipulator during in a fast maneuver. The strategy is as follows: high-bandwidth local PD gains are used during the manipulator's fast motion to insure the desired trajectory in joint space. Then, upon completion of the trajectory, the manipulator is placed under P-PED control (in real time) to damp out any residual vibration resulting from this motion.

Figure 10 shows the initial and final configurations of the manipulator for this experiment. This maneuver was executed both, under conventional PD control and switching to P-PED control at the end of the ma-

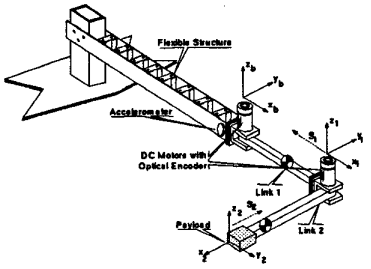

Figure 8: The MIT Elastic Base Manipulator Testbed (MIT-EBM)

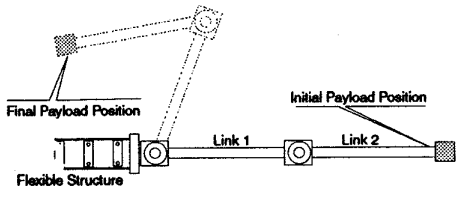

Figure 9: Initial and Final Configuration of the MIT-EBM

neuver. The results are shown in Figure 11 in the form of the time history of the manipulator base position during and after the maneuver. Notice that for this particular system the P-PED method reduced the time of completion of the maneuver from 6 second to 4 seconds when compared to using the nominal PD gains after the maneuver.

4 P-PED Evaluation for a Spatial System

The P-PED method presented here so far has been experimentally evaluated for planar systems only, due to limitations imposed by gravity. The problem of spatial testing of micro-gravity algorithms in one-g have been addressed in [9] with some degree of success. However, the P-PED method has been extensively evaluated in simulation for a spatial system and found to be very promising. For example, consider the 5-DOF manipulator mounted on a flexible structure as shown in Figure 12. This system incorporates the dynamic characteristics of an experimental robotic arm currently under design as part of the NASA's InStep project entitled *Microgravity Manipulator Dynamic Experiment.* This is research project is been

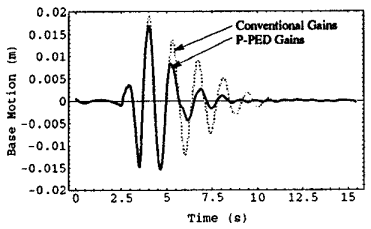

Figure 10: MIT-EBM Base Residual Vibrations: Manipulator Joints Under Conventional PD Control and Under P-PED Control

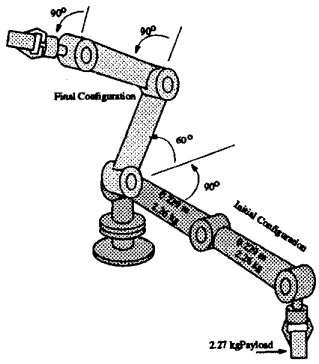

Figure 11: The 5-DOF Model Used In Simulation Including Initial and Final Configuration Used in Evaluation

developed by MIT, The University of Puerto Rico-Mayaguez, Martin Marietta Co. and NASA Langley Research Center.

The simulation presented here are designed to evaluate the effectiveness of the P-PED method in damping residual structural vibrations resulting from the moving of the manipulator. For this simulation, the manipulator was assumed supported by a flexible structure defined by a stiffness matrix that, when combined with the mass and inertia of the manipulator at a given configuration, results in a natural frequency of 1 hz in each of the base six directions of motion, i.e., three translations and three rotations.

Two scenarios presented. In the first, a high-bandwidth local PD gains is used during and after a given 0.7 seconds maneuver. In the second simulation, high-bandwidth local PD gains were used during the given 0.7 seconds maneuver but, upon completion of the trajectory, the manipulator was switched (in real-time) to P-PED control to damp out the residual vibrations resulting from this maneuver.

The results of this simulation are presented in Figure 13 which shows the history of the strain energy accumulated in the system's supporting structure for each of the two simulation runs. The strain energy accumulated in the system's supporting structure is plotted instead of three translations and three orientations to simplify the visualization and analysis of the results. Notice that when the system was placed under P-PED control (dark line) it was able to damp out all the residual strain energy in 5 seconds, compared with more than 10 seconds using conventional PD control.

5 Conclusion

This paper presents the Pseudo-Passive Energy Dissipation method for reducing structural vibrations in an elastically-mounted long-reach space manipulator system. This method is based on tuning the manipulator's closed loop gains so as to increase the transfer of energy from the manipulator's flexible (and very lightly damped) supporting structure to its actuators. This energy is then dissipated by the actuators, which are commanded to behave as passive linear springs and dampers. This paper also shows a

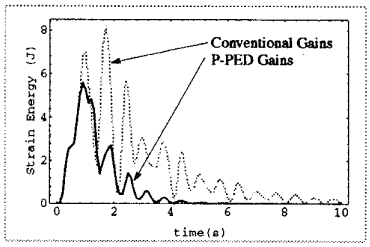

Figure 12: 5-DOF Spatial System Strain Energy History. Using Conventional PD and P-PED.

method for computing the optimal P-PED gains for a general n-DOF manipulator. Numerical as well as experimental results demonstrate the effectiveness of this method.

Acknowledgements

The support of this work by NASA Langley Research Center Automation Branch, and Martin Marietta Aerospace, Denver, Colorado, is acknowledged.

6 References

[1] Asada, H., and Slotine, J.J.E., *Robot Analysis and Control.* John Wiler and Songs, New York, NY, 1986.

[2] Book, W., "Structural Flexibility of Motion Systems in Space Environment," IEEE Transactions on Robotics and Automation, 5, pp. 524-530, 1993

[3] Bronez, M.A., Clarke, M.M., and Quinn, A., Requirements Development for a Free-Flying Robot-The 'ROBIN', *Proceedings 1986 IEEE International Conference in Robotics and Automation*, Apr. 7-10, 1986, San Francisco, CA, pp. 667-672.

[4] Cleary, K., Nguyen, L., and Frisch, H., *A demonstration of Vibration Reduction for a Flexible Beam Using Input Shaping,* Proceedings of the 1992 IEEE/RSJ International Conference on Intelligent Robots and Systems, July 7-10, Raleigh, North Carolina.

[5] Corrigan, T., The Development and Application of Methods for Emulating Micro-gravity, *Master Thesis, Department of Mechanical Engineering, MIT, Cambridge,* MA, August 1994.

[6] Crane, C.D., Duffy, J., and Carnahan, T., A Kinematic Analysis of the Space Station Remote Manipulator System (SSRMS), *Journal of Robotic Systems,* 8(5), pp. 637-658, 1991.

[7] Dorf, R.C., *Modern Control Systems,* Fifth Edition, Addison Wesley, New York, NY,1989

[8] Dubowsky, S., *Space Robotics: Dynamics and Control,* Published by Kluwer Academic Publishers, Norwell, MA, 1993, Xu and Kanade - Editors.

[9] Dubousky, S., Durfee, W., Corrigan, T., Kuklinsky, A., and Muler, U., "A Laboratory Test Bed for Space Robotics: The VES Mod II, "IROS '94 International Conference on Intelligent Robotics and Systems, September 12-16, 1994, Munchen, Germany.

[10] Dubowsky, S., and Papadopoulos, E., "The Kinematics, Dynamics and Control of Free-Flying and Free-Floating Space Robotic Systems," *Special Issue on Space Robotics, IEEE Transactions on Robotics and Automation. Vol. 9, No. 5, October 1993, pp 1-13. (Invited)*

[11] Erb, G. Canada's Mobile Servicing System Space Technology, *Vol. 10, No. 1/2, 1990, pp. 19-25.*

[12] Hootsmans, N.A.M., and Dubowsky, S., The Experimental Performance of a Motion Manipulators Control Algorithm, Proceedings 1992 IEEE international Conference on Robotics and Automation, *Nice, France, May, 10-15, 1992.*

[13] Hunter, D., " The Space Station Servicing System," Proc. of the 1994 Artificial Intelligence, Robotics and Automation in Space Conference, (i-SAIRAS-94), Pasadena, CA, 1994.

[14] Meckl, P., and Seering, W., Minimizing Residual Vibration Point-to-Point motion. ASME Journal of Vibration, Acoustics, Stress, and Reliability in Design, *107(4):378-382,October 1985.*

[15] Mori, H., Iwata, T., and Oda, M., " An Overview of Japan's Space Automation and Robotics Activities," Proc. 1992 Artificial Intelligence, Robotics and Automation in Space, Toulouse, France, 1993, pp. 19-24

[16] Schmitz, E., " CSI- Related Dynamics and Control Issues in Space Robotics, "Proceedings of the 5th Controls-Structures interaction (CSI) Technology, March 3-5, 1992, Lake Tahoe, Nevada.

[17] Singer, N., Residual Vibration Reduction in Computer Controlled Machines, Ph.D. Thesis, Mechanical Engineering Department, MIT, *January, 1989.*

[18] Spoford, J., and Hause, C. E., NASA In-Step Proposal: Microgravity Manipulator Dynamic Experiment, Technical report, Martin Marietta Astronautics Group, Intelligent Systems/Advanced Controls, January, 1993

[19] Torres, M. A., Modeling, Path-Planning and Control of Space Manipulators: The Coupling Map Concept, Ph.D. Thesis, Department of Mechanical Engineering, MIT, Cambridge, *MA, February 1993.*

[20] Torres, M.A., and Dubowsky, S., Path-Planing for Elastically Constrained Space Manipulator Systems," In Proceedings of the IEEE International Conference on Robotics and Automation, *Atlanta, GA, May 2-7, 1993.*

[21] Torres, M.A., Dubowsky, S., and Pissoni, A., " Path Planning for Elastically Mounted Space Manipulators: Experimental Evaluation of the Coupling Map," Proc. of the 1994 IEEE International Conference on Robotics and Automation, San Diego, CA, pp. 2227-2233, May 10-12, 1994.

[22] Vaza, Z., and Dubowsky, S., The Kinematics, Dynamics and Control of Space Manipulators: The Virtual Manipulator Approach. The International Journal of Robotics Research, *9(4):3-21, August, 1990*

[23] Waltz, D., On-Orbit Servicing of Space Systems, Krieger Pub. Co., Fl., 1993